JACS
JOURNAL OF THE AMERICAN CHEMICAL SOCIETY

ARTICLE

pubs.acs.org/JACS

Facet-Dependent and Au Nanocrystal-Enhanced Electrical and Photocatalytic Properties of Au−Cu_2O Core−Shell Heterostructures

Chun-Hong Kuo,[†,§] Yu-Chen Yang,[‡,§] Shangjr Gwo,[*,‡] and Michael H. Huang[*,†]

[†]Department of Chemistry and [‡]Department of Physics, National Tsing Hua University, Hsinchu 30013, Taiwan

Supporting Information

ABSTRACT: We report highly facet-dependent electrical properties of Cu_2O nanocubes and octahedra and significant enhancement of gold nanocrystal cores to the electrical conductivity of Au−Cu_2O core−shell octahedra. Cu_2O nanocubes and octahedra and Au−Cu_2O core−shell cubes and octahedra were synthesized by following our reported facile procedures at room temperature. Two oxide-free tungsten probes attached to a nanomanipulator installed inside a scanning electron microscope made contacts to a single Cu_2O nanocrystal for the $I-V$ measurements. Pristine Cu_2O octahedra bounded by {111} facets are 1100 times more conductive than pristine Cu_2O cubes enclosed by {100} faces, which are barely conductive. Core−shell cubes are only slightly more conductive than pristine cubes. A 10 000-fold increase in conductivity over a cube has been recorded for an octahedron. Remarkably, core−shell octahedra are far more conductive than pristine octahedra. The same facet-dependent electrical behavior can still be observed on a single nanocrystal exposing both {111} and {100} facets. This new fundamental property may be observable in other semiconductor nanocrystals. We also have shown that both core−shell cubes and octahedra outperform pristine cubes and octahedra in the photodegradation of methyl orange. Efficient photoinduced charge separation is attributed to this enhanced photocatalytic activity. Interestingly, facet-selective etching occurred over the {100} corners of some octahedra and core−shell octahedra during photocatalysis. The successful preparation of Au−Cu_2O core−shell heterostructures with precise shape control has offered opportunities to discover new and exciting physical and chemical properties of nanocrystals.

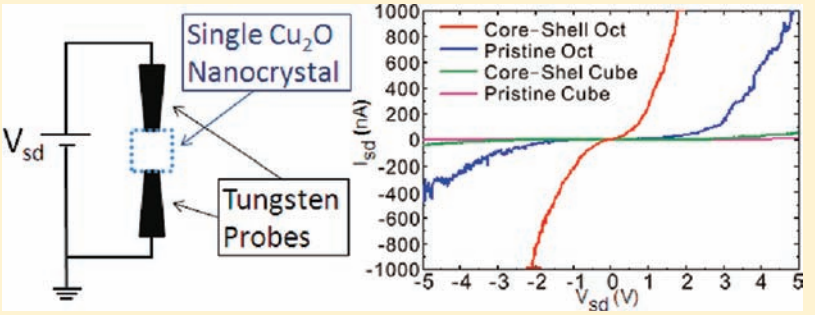

INTRODUCTION

The growth of metal and semiconductor nanocrystals with well-defined morphologies such as cubic, octahedral, and rhombic dodecahedral structures is not only synthetically interesting, but the resulting nanocrystals also offer opportunities for the investigation of their facet-dependent catalytic, photocatalytic, molecular adsorption, and other surface-related properties.[1,2] If their dimensions are monodisperse and can be well controlled to tens of nanometers, they may readily form self-assembled structures.[3−6] Ordered assembly of these metal nanocrystals can present novel plasmonic properties. An interesting physical property of these shape-controlled nanocrystals that has never been explored is their facet-dependent electrical property. Although many studies have performed the electrical transport measurements of individual nanowires, such measurements on single nanocrystals are rare.[7−9] The successful preparation of semiconductor nanocrystals with these distinct shapes and different surfaces enables the examination of their electrical properties with respect to the surface facets. The results can be very interesting and important if large conductivity differences were recorded.

We have previously developed a facile method for the synthesis of cuprous oxide (Cu_2O) crystals in aqueous solution with systematic shape evolution from cubic to octahedral and hexapod structures.[10−12] Shape control was achieved simply by varying the amount of reductant $NH_2OH\cdot HCl$ used. Cu_2O is a p-type semiconductor with a direct band gap of 2.17 eV. By introducing octahedral gold nanocrystals into the same solutions for the growth of cubic and octahedral Cu_2O crystals, Au−Cu_2O core−shell heterostructures with cubic to octahedral morphologies can be easily synthesized.[13] The Au cores have a precise orientation relationship with the Cu_2O shells. These heterostructures represent one of the first metal−semiconductor systems with well-defined shapes for both the cores and the shells. It would be interesting to investigate the electrical properties of these Cu_2O nanocubes and octahedra with and without the incorporation of Au nanocrystal cores. The nanocubes and octahedra are bounded by largely {100} and {111} facets, respectively. Electrical transport measurements with probes contacting only a specific crystal face can reveal the presence of any facet-dependent electrical properties of Cu_2O crystals. Furthermore, one can see how the gold nanocrystal cores improve electrical transport in the core−shell heterostructures.

Received: October 13, 2010
Published: December 21, 2010

dx.doi.org/10.1021/ja109182y | J. Am. Chem. Soc. 2011, 133, 1052–1057

Our study shows that the electrical properties of Cu_2O crystals are highly facet-dependent and that the Au nanocrystal cores can dramatically enhance conductivity of the octahedral Au−Cu_2O core−shell heterostructures. The results are quite exciting and suggest that semiconductor crystal facets should be exploited in the fabrication of nanoscale electronic devices.

In addition to the observation of facet-dependent and Au nanocrystal-enhanced electrical properties of Cu_2O nanocrystals, their photocatalytic activity also exhibits the same facet-dependent and Au-enhanced effects. Remarkably facet-dependent photocatalytic activity of Cu_2O crystals has also been demonstrated recently.[11] Octahedra and hexapods with mainly {111} exposed facets were found to photodecompose negatively charged methyl orange molecules, while perfect cubes bounded by exclusively {100} faces were photocatalytically inactive. This dramatic difference is related to the surface atoms; the copper atom-terminated {111} faces of Cu_2O are expected to interact more favorably with negatively charged molecular species.[2,11,14] The same surface property has been observed in Ag_2O crystals.[15] It should be interesting to see if the Au−Cu_2O core−shell heterostructures show enhanced photocatalytic activity. Photoinduced charge separation in core−shell heterostructures should be more efficient than in pure semiconductor nanocrystals, leading to an enhanced photocatalytic activity.[16,17] Significant enhancements in the photocatalysis performance of the Au−Cu_2O core−shell heterostructures have indeed been observed.

EXPERIMENTAL SECTION

Growth of Cu_2O Nanocrystals and Au−Cu_2O Core−Shell Heterostructures. Cu_2O nanocrystals and Au−Cu_2O core−shell heterostructures were synthesized by following our reported procedures.[10−12] The procedures are almost identical and easy to follow. To make the core−shell heterostructures for this study, one just needs to add octahedral gold nanocrystals into a solution mixture for growing Cu_2O nanocubes and octahedra. The octahedral gold nanocrystals with sizes of ∼90 nm were prepared using our reported hydrothermal synthesis approach.[4] In a typical synthesis of the Au−Cu_2O core−shell heterostructures, 9.4 mL (for nanocubes) or 8.9 mL (for octahedra) of deionized water, 0.1 mL of 1×10^{-3} M $CuCl_2$ solution, 0.087 g of sodium dodecyl sulfate (SDS), 0.1 mL of the concentrated octahedral gold nanocrystal solution, and 0.25 mL of 1 M NaOH were introduced into a sample vial in the order listed. Next, 0.15 mL (for nanocubes) or 0.65 mL (for octahedra) of 0.2 M $NH_2OH \cdot HCl$ was added. The total solution volume is 10 mL. After the addition of $NH_2OH \cdot HCl$, the solution color became yellow and finally light brown by aging the mixture for 2 h. To collect the products, the solution was washed with deionized water and centrifuged four times at 3000 rpm for 5 min to remove the surfactant. The precipitate was dispersed in 0.5 mL of ethanol.

Electrical Property Measurements of Single Nanocrystals. A tiny drop of Cu_2O nanocrystal solution in ethanol was added to a silicon substrate and dried. The substrate was loaded into a field-emission scanning electron microscope (FE-SEM, Zeiss Ultra 55) with a four-probe nanomanipulator (Zyvex S100) installed inside the FE-SEM. For this study, two tungsten probes mounted on the nanomanipulator were used to pick up a single Cu_2O nanocrystal from the substrate and measure its $I-V$ characteristics. A Keithley 2400 sourcemeter connected to the tungsten probes was used to make the electrical measurements. Tungsten probes were used as electrodes instead of the employment of noble metal electrodes because the tungsten probe fabrication process is well-known and the probes are likely stronger. Before the measurements, the surface oxide layer of the tungsten probes need to be removed by Joule heat, as the native oxide can affect the measurements. The two tungsten probes first made tip-to-tip contact to each other by controlling the nanomanipulator. Next, a sweep voltage from 0 to 8 or 10 V was increasingly applied with the current limited to 150 μA to prevent over welding. At the beginning, the $I-V$ curves across the two probes showed a retarded behavior because of the native oxide formed spontaneously on the tungsten surface after an electrochemical etching process to make the probes. The high contact resistance at the interface of the two tungsten probes with an oxide layer on the surface will result in a locally high temperature by Joule heat. This heating can weld the probes and remove the native oxide layer. The two tips will stick to each other when they are melted by Joule heat and form a flat end when carefully pulled by the nanomanipulator to separate them. To confirm the oxide layer was removed, the voltage was swept many times until the $I-V$ curve across the two contact probes became linear and the resistance was around 20 Ω. After current annealing of the tungsten probes, one probe touched a single Cu_2O nanocrystal and moved it to the right orientation. The electrostatic force present between the probe and nanocrystal can remove the crystal away from the Si substrate and suspend the particle in the FE-SEM chamber. This step is necessary to avoid any leakage current from Cu_2O to the Si substrate. After picking up the nanocrystal, a second probe touched the crystal from the other side at the right face. While performing the electrical measurements, we blocked out the electron beam to rule out the influence of electron bombardment and charging effect. The whole $I-V$ measurements of Cu_2O nanocrystals were carried out in the FE-SEM chamber with high vacuum of about 5×10^{-6} Torr at room temperature.

Photocatalytic Activity Measurements. To obtain a sufficient amount of nanocrystals for photocatalytic activity measurements, the amounts of reagents used in the procedure described above were increased 10-fold. The particle powder was gathered by centrifugation at 3000 rpm for 5 min five times (deionized water for the first run and ethanol for the other runs) and dried (see Figure S4 for the photographs of the four nanocrystal samples). Next, surface areas of the four powder samples were determined through nitrogen adsorption−desorption isotherms at 77 K using a Quantachrome Nova 2000e analyzer. The surface areas of Cu_2O nanocubes, octahedra, core−shell cubes, and core−shell octahedra were found to be 8, 5, 6, and 5 m^2/g, respectively. The synthesized amounts of Cu_2O nanocubes, octahedra, core−shell cubes, and core−shell octahedra samples weighed 2.4, 3.1, 2.9, and 3.2 mg, respectively. The entire amount of each powder sample was dispersed in 90 mL of 15 mg/L methyl orange aqueous solution contained in a homemade quartz holder.[11] The holder was irradiated with light from a 500 W Xe lamp placed 25 cm away, and the solution was vigorously stirred. UV−vis spectra of a few milliliters of the solution were taken before and after every 60 min of photoirradiation to determine the amount of methyl orange decomposed.

RESULTS AND DISCUSSION

The Cu_2O nanocrystals and Au−Cu_2O core−shell heterostructures were synthesized by following our reported procedures. By varying the amount of reductant introduced, both pristine and core−shell crystals with systematic shape evolution from cubic to cuboctahedral, truncated octahedral, and octahedral structures can be prepared. For facet-dependent electrical property measurements, cubes and octahedra were selected because they are bounded by largely {100} and {111} faces, respectively. Two tungsten probes attached to a nanomanipulator installed inside a field-emission scanning electron microscope (FE-SEM) were first contacted, and a voltage was applied to thermally remove the native oxide layer on the probes. The probes were then pulled apart and can form flat tips (see Figure S1 of the Supporting Information). One probe made contact with a crystal and lifted it above the underlying silicon substrate

dx.doi.org/10.1021/ja109182y |J. Am. Chem. Soc. 2011, 133, 1052–1057

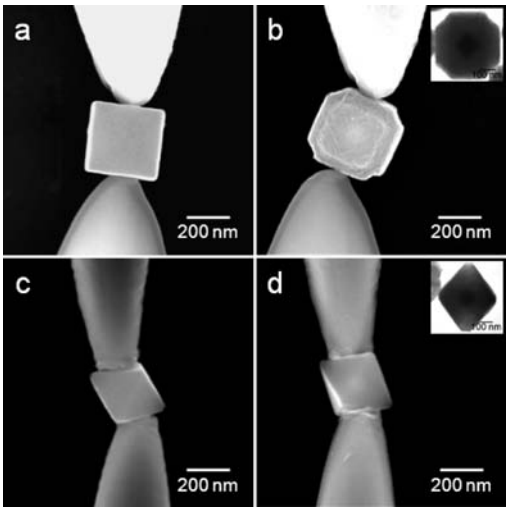

Figure 1. FE-SEM images showing two tungsten probes in contact with a single Cu_2O nanocrystal for $I-V$ measurements. (a) Pristine Cu_2O nanocube. (b) Au−Cu_2O core−shell nanocube. The bright spot at the center of the particle is the gold core. Inset shows the corresponding TEM image of the particle. The octahedral gold nanocrystal core is precisely positioned such that its corners are directed perpendicularly to the {100} faces of the nanocube. (c) Pristine Cu_2O octahedron. (d) Au−Cu_2O core−shell octahedron. Inset shows the corresponding TEM image of the particle. The gold core has the same orientation as the Cu_2O shell.

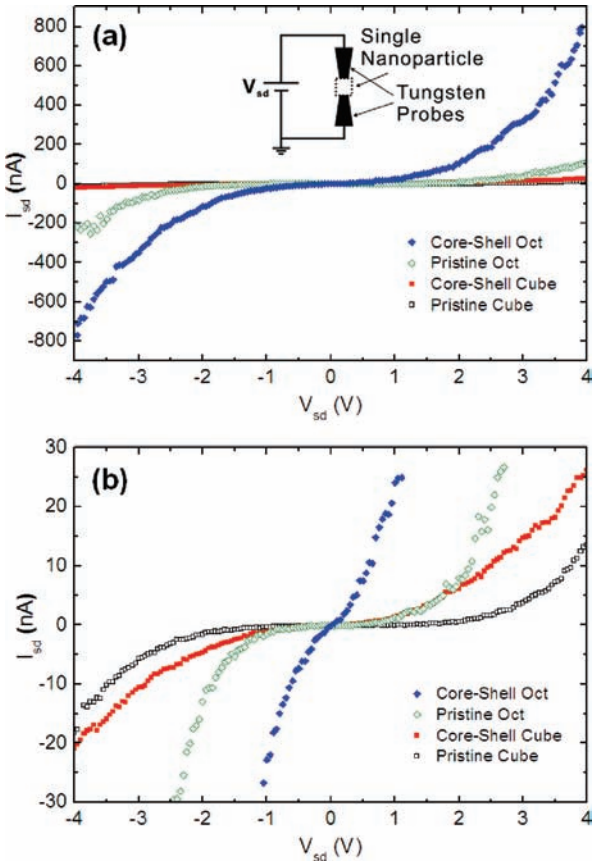

Figure 2. Room temperature $I-V$ curves of single Cu_2O nanocrystals. The $I-V$ curves were obtained using the following single nanoparticles: Au−Cu_2O core−shell octahedron (blue ◆), Cu_2O octahedron (green ◇), Au−Cu_2O core−shell nanocube (red ■), and Cu_2O nanocube (□). The inset in panel a is a schematic diagram of the measurement circuit. (b) An expanded plot to see the $I-V$ curves for the cube and core−shell cube. The $I-V$ curves show the Au−Cu_2O core−shell octahedron is far more conductive than the other nanocrystals.

via electrostatic force.[18] The other probe was then attached to this crystal. Figure 1 gives SEM images of the probes touching the four different Cu_2O crystals examined in this study. The crystals have similar sizes in the range of 350−420 nm. Here, one set of probes was used to measure the $I-V$ curves of a single Cu_2O cube and core−shell cube. The Au−Cu_2O core−shell cubes are corner- and edge-truncated, and the {100} faces can be slightly raised. Another set of probes was fabricated to perform the measurements on an octahedron and a core−shell octahedron with the probes touching the {111} facets. A new set of probes needs to be made each time a new sample is loaded into the electron microscope to ensure that reliable data are obtained.

Figure 2 presents the $I-V$ curves obtained from the four different Cu_2O nanocrystals shown in Figure 1. Symmetric electrical response has been recorded for each sample. The nonlinearity of these $I-V$ curves is caused by the Schottky barriers formed between the semiconductor nanoparticles and tungsten probes in our measurement system. The Schottky barriers formed at the two interfaces are attributed to the work function difference between the p-type Cu_2O (4.84 eV)[19] and tungsten probes (4.5 eV). Both the cube and the core−shell cube show much lower conductivity than the octahedron. In fact, the Cu_2O cube is barely conductive even at an applied voltage of 3 V. The gold core only improves the conductivity of the core−shell cube slightly. Remarkably, the core−shell octahedron displays a much higher electrical conductivity behavior than do all other crystals. A measured current of 800 nA at 4 V for the core-shell octahedron is around 8, 32, and 60 times larger than those of the octahedron, the core−shell cube, and the cube, respectively. The results reveal for the first time that the electrical properties of Cu_2O nanocrystals are highly facet-dependent; the {111} faces of Cu_2O nanocrystals are far more electrically conductive than the {100} faces. Furthermore, the incorporated gold cores in the Au−Cu_2O core−shell octahedra can dramatically enhance the electrical conductivity of the nanocrystals. These observations are quite significant and profound, as other semiconductor nanocrystals may also exhibit such strongly facet-specific electrical properties. Small differences in the electrical current values have been measured over different side facets of a single CuO nanowire.[20] The observation of such large facet-dependent electrical properties in Cu_2O crystals is surprising. A 100 000-fold increase in the conductance of individual CdSe nanorods with Au tips on the nanorod ends, as compared to CdSe nanorods without the Au tips, has been measured.[21] However, this large conductance difference is not related to the surface facets of the CdSe nanocrystals.

When the same set of probes was used to measure the $I-V$ curves of Cu_2O cubes and octahedra, more drastic conductivity differences may be recorded (Figure S2). The comparison of their $I-V$ response can also be more accurate. With the probes touching the opposite {100} faces of a pristine Cu_2O cube, the measured current is only 4 nA at an applied voltage of 3 V. Surprisingly, the current can reach over 4000 nA at the same voltage when the same probes touched opposite {111} faces of an octahedron. The current difference is more than 1100 times. In another measurement using the same octahedron, but with the

dx.doi.org/10.1021/ja109182y |*J. Am. Chem. Soc.* 2011, 133, 1052–1057

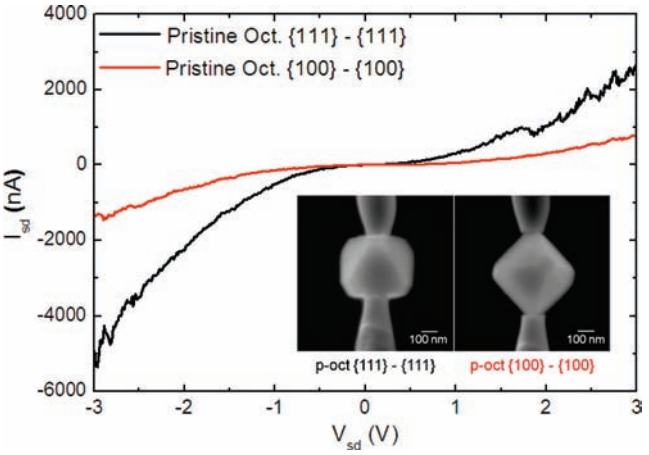

Figure 3. $I-V$ curves of the same Cu_2O octahedron with the probes contacting either only the {111} faces or only the {100} corners. Both $I-V$ measurements of the Cu_2O octahedron were carried out using the same set of tungsten probes. Significant differences in conductivity exist even in the same nanocrystal depending on where the electrical contacts are made. A larger octahedron was chosen for the measurements.

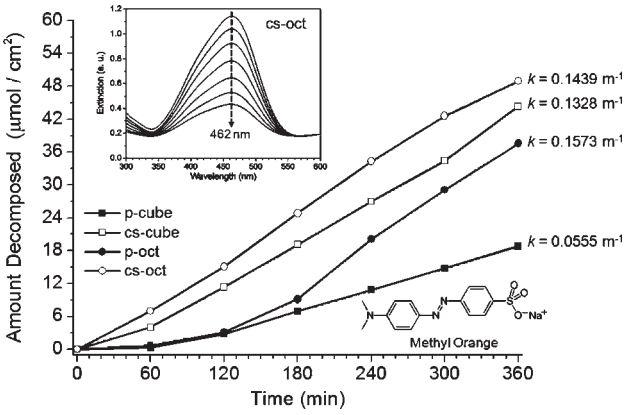

Figure 4. A plot of the amount of methyl orange photodecomposed versus time using pristine Cu_2O and Au−Cu_2O core−shell nanocrystal catalysts. Molecular structure of methyl orange is given. The reactions closely follow first-order reaction kinetics after the first hour except for pristine octahedra. Their rate constants are provided. The rate of photodegradation reaction by octahedra speeds up gradually and becomes constant. Photocatalytic activity is obviously enhanced for the Au−Cu_2O core−shell heterostructures. Inset shows UV−vis absorption spectra of methyl orange as a function of irradiation time using Au−Cu_2O core−shell octahedra as the photocatalysts.

probes possibly partially touching the edge of the octahedron, the current rapidly increases to 10 000 nA at a voltage of just below 2.4 V. At this point, the current difference can be 10 000-fold. The results further indicate that the difference in electrical conductivity between {111} faces and {100} faces of Cu_2O nanocrystals is enormous. A more drastic conductivity difference can be expected for the Au−Cu_2O core−shell cubes and octahedra. Using a different set of tungsten probes for the measurements, a core−shell octahedron easily reaches a current of 1000 nA at 1.9 V, while a pristine octahedron needs an applied voltage of 5 V to get to this current value. A core−shell cube displays the same $I-V$ response as that shown in Figure 1 using these same probes.

Similar facet-dependent conductivity behavior can still be observed in the same nanocrystal. Figure 3 presents the $I-V$ curves of the same Cu_2O octahedron with the same probes touching either only the {111} faces or only the {100} corners. Although the current measured at 3 V with the probes contacting the {100} faces is significantly higher than that obtained for the cubes, the {111} faces of the octahedron still show roughly 3.5 times higher current than that of the {100} faces. The probe tips cover the entire {100} faces of the octahedron. Charge carriers may easily move to adjacent {111} faces with a lower barrier, thereby increasing the observed conductivity of the {100} faces. Use of much smaller tips may restore the large conductivity difference seen in Figure S2. The results imply that one can utilize a single Cu_2O nanocrystal as a key electronic component such as in the fabrication of a field-effect transistor by forming electrical connections to different facets of a single crystal. So the logical next experiment to perform may be the demonstration of maintenance of this facet-dependent electrical conductivity behavior with the nanocrystals deposited on the substrates. Work in this direction is in progress.

The pronounced facet-dependent electrical behavior of Cu_2O nanocrystals is an unexplored research topic. Its implication can be far-reaching as the phenomena can be general and observable in other semiconductors. The poor electrical conductivity through the {100} faces of Cu_2O crystals is not due to possible surfactant adsorption, as surfactant has been removed through repeated centrifugation of nanocrystals and dispersion in ethanol. Sodium dodecyl sulfate (SDS) used in the synthesis of these nanocrystals has been shown to selectively deposit onto the {111} faces of Cu_2O crystals.[2] Any residual surfactant coverage would lower the electrical conductivity of the {111} faces. This may reverse the $I-V$ characteristics for the two different facets and is therefore not an explanation for the observed electrical behavior. Another consideration concerns the transport pathway of the charge carriers. The fact Au−Cu_2O core−shell octahedra are much more electrically conductive suggests that the charge carriers move across the interior of the nanocrystals rather than along the particle surfaces. The Au nanocrystal core provides a conduction pathway to greatly enhance the conductivity of the core−shell octahedra. Cu_2O has an isotropic or symmetric crystal structure. There is no preferred pathway or direction for carrier transport. Thus, the large facet-dependent electrical response of these Cu_2O nanocrystals is likely a surface effect. The barrier for charge transport at the junction between the {100} faces of Cu_2O and the tungsten probe is substantially higher than that for the {111} faces. Further study is necessary to understand why surface atomic arrangements and perhaps electronic structures of Cu_2O at the surface can have such a pronounced effect on the electrical conductivity of the crystals.

In addition to the electrical property characterization of these Cu_2O crystals, another surface-related property we would like to investigate is whether the gold nanocrystal cores can enhance the photocatalytic activity of Cu_2O cubes and octahedra. Previously, we have demonstrated that octahedra bounded by {111} faces are active toward the photodegradation of methyl orange, while perfect cubes bounded by entirely {100} faces are not.[11] The negatively charged methyl orange molecules adsorb preferentially to the {111} faces with exposed copper atoms possibly via electrostatic interactions.[11] To carefully compare the relative photocatalytic activity of the cubes, octahedra, core−shell cubes, and core−shell octahedra per unit area, a sufficiently large amount of nanocrystals was prepared for each sample and weighted (Table S1 and experimental section in the Supporting

dx.doi.org/10.1021/ja109182y |J. Am. Chem. Soc. 2011, 133, 1052–1057

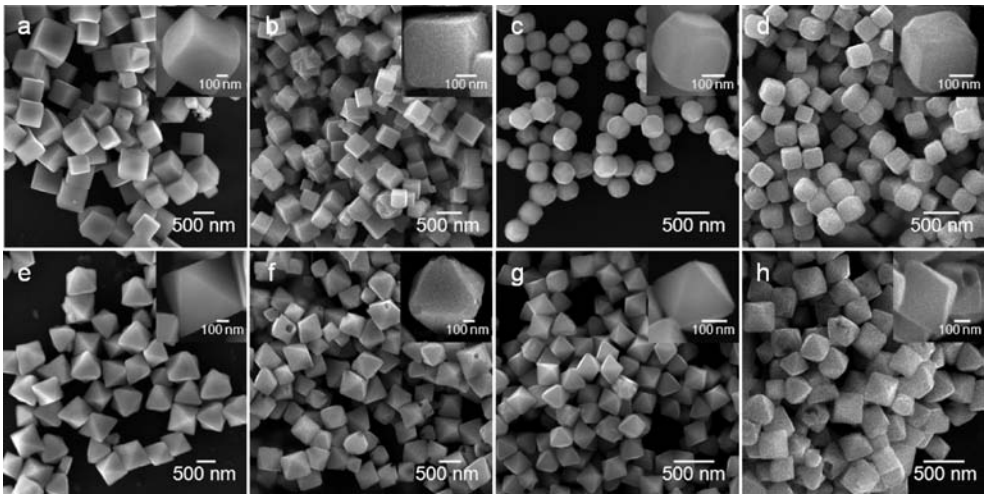

Figure 5. SEM images of the Cu_2O nanocrystals before and after photodegradation of methyl orange molecules. (a,e) Pristine Cu_2O crystals. (c,g) Au−Cu_2O core−shell heterostructures. In the cases of pristine cubes and core−shell cubes, their morphologies before (a,c) and after (b,d) the photocatalysis experiment remain the same. It is evident that the pristine cubes are almost perfect cubes, while the core−shell cubes are edge- and corner-truncated cubes. For octahedra and core−shell octahedra, they have a perfect octahedral structure before the reaction (e,g). After the photocatalysis experiment (f,h), some of the particles exhibit slightly etched corners.

Information). Surface areas of the cubes, octahedra, core−shell cubes, and core−shell octahedra were determined from nitrogen adsorption−desorption isotherm measurements. The entire amount of the nanocrystal powder was used for the photodegradation experiment. Figure 4 gives a plot of the amount of methyl orange decomposed as a function of irradiation time using pristine Cu_2O and Au−Cu_2O core−shell nanocrystal catalysts. The results show that core−shell octahedra and core−shell cubes outperform pristine octahedra and cubes in the photodegradation of methyl orange. The reason pristine cubes still show some photocatalytic activity is related to their truncated corners. The core−shell cubes are edge- and corner-truncated, exposing {110} and {111} surfaces. The {110} facets of Cu_2O have been shown to be more photocatalytically active than the {111} facets due to their higher surface energy and greater density of copper dangling bonds.[22] After 6 h of irradiation, the values of decomposed methyl orange are, respectively, 18.8, 37.6, 44.4, and 49.0 μmol/cm^2 for cubes, octahedra, core−shell cubes, and core−shell octahedra. It was found that the decomposition rates of these crystals generally follow first-order reaction kinetics. For pristine octahedra, the reaction rate is slow in the first 2 h and speeds up afterward. The rate constants of cubes, octahedra, core−shell cubes, and core−shell octahedra are 0.056, 0.157, 0.133, and 0.144 min^{-1}, respectively. Rate constants for pristine cubes and octahedra were obtained using data points from the second hour. Incorporation of Au nanocrystal cores evidently enhances the photocatalytic activity of both Cu_2O cubes and octahedra. The photoexcited electrons from Cu_2O are likely to move to the Au core, while holes migrate to the surface.[17] This efficient charge separation process significantly enhances the photocatalytic activity of the core−shell cubes and octahedra. The results also suggest that Au−Cu_2O core−shell nanocrystals are better candidates than pristine Cu_2O crystals for catalyzing other reactions.

SEM images of the four Cu_2O nanocrystal samples before and after the photodegradation experiments were taken using a JEOL 7000F scanning electron microscope to examine their morphologies (Figure 5). No noticeable changes have been found for the pristine cubes and core−shell cubes after 6 h of photocatalysis. Interestingly, some octahedra and core−shell octahedra show etched corners after the photodegradation reaction. Pristine octahedra appear to have more corners etched than core−shell octahedra do. Figure 1 reveals that some pristine octahedra and core−shell octahedra possess tiny truncated {100} corners. Facet-selective oxidative or acid etching is an interesting aspect of nanometerials research that is relatively unexplored, yet it offers a convenient route to the preparation of hollow nanocages and nanoframe structures.[23,24] X-ray diffraction patterns of the four Cu_2O nanocrystal samples taken after the photodegradation experiments give only reflection peaks of Cu_2O (and Au in the cases of core−shell cubes and octahedra), indicating that CuO was not formed (Figure S3).[25] Their colors also suggest no formation of CuO (Figure S4). It is unclear why selective {100} facet etching only occurs on Cu_2O octahedra but not on cubes. The large {100} surface area of the cubes can make this etching process be unapparent. Although the phenomenon may suggest that corners of Cu_2O octahedra are more reactive, core−shell cubes are equally effective at photodecomposing methyl orange. It is also not certain how this etching process would eventually affect the durability of core−shell octahedra as the most efficient catalysts. Explanation for this face-selective oxidative etching requires further investigation. This study illustrates the importance of being able to precisely control and vary the shell morphology in the fabrication of Au−Cu_2O core−shell heterostructures. While core−shell octahedra are most desirable for their excellent electrical conductivity properties, use of core−shell cubes for photocatalytic reactions may be advantageous for their better stability and good performance.

■ CONCLUSION

In summary, we have demonstrated that the electrical behavior of Cu_2O crystals is highly facet-dependent and that gold nanocrystal cores can significantly enhance the conductivity of Au−Cu_2O core−shell octahedra. $I-V$ characteristics of the Cu_2O nanocrystals were carried out in the sample chamber of

a FE-SEM with tungsten probes making contact to the crystals and show symmetric response. Using the same set of probes, Cu_2O octahedra bounded by {111} faces have been found to be 1100 times more conductive than Cu_2O cubes enclosed by {100} surfaces. A 10 000-fold increase in conductivity has also been recorded. Cu_2O cubes are barely conductive. Au−Cu_2O core−shell octahedra are even more conductive than pristine Cu_2O octahedra. The same facet-dependent electrical response can still be measured on a single octahedron with slightly truncated {100} corners. This discovery is significant not only because this is new fundamental physics of Cu_2O nanocrystals. The implication may be far-reaching as this large facet-dependent electrical property can be quite general for many other semiconductor nanocrystals. In addition, we have shown that both Au−Cu_2O core−shell cubes and octahedra outperform pristine Cu_2O cubes and octahedra in the photodegradation of methyl orange. The gold nanocrystal cores can substantially enhance the photocatalytic activity of the core−shell heterostructures via efficient charge separation. Facet-selective etching has occurred at the corners of some Cu_2O octahedra and core−shell octahedra during photocatalysis, while morphologies of cubes and core−shell cubes remain unaltered. This study demonstrates that new and exciting physical and chemical properties of nanocrystals can be discovered through the preparation of single- and multicomponent nanostructures with well-controlled morphologies and facets.

■ ASSOCIATED CONTENT

Supporting Information. Detailed experimental procedures, SEM images of the tungsten probes before and after current heating, *I*−*V* curves of single pristine Cu_2O octahedron and nanocube measured with the same set of probes, weights, total surface areas, and photographs of the nanocrystal samples used, and XRD patterns. This material is available free of charge via the Internet at http://pubs.acs.org.

■ AUTHOR INFORMATION

Corresponding Author

gwo@phys.nthu.edu.tw; hyhuang@mx.nthu.edu.tw

Author Contributions

[§]These authors contributed equally to this work.

■ ACKNOWLEDGMENT

This study was supported by the National Science Council of Taiwan (Grants NSC 98-2113-M-007-005-MY3, NSC 99-2120-M-007-004, and NSC 98-2811-M-007-066).

■ REFERENCES

(1) Bratlie, K. M.; Lee, H.; Komvopoulos, K.; Yang, P.; Somorjai, G. A. *Nano Lett.* **2007,** *7*, 3097.
(2) Read, C. G.; Steinmiller, E. M. P.; Choi, K.-S. *J. Am. Chem. Soc.* **2009,** *131*, 12040.
(3) Tao, A.; Sinsermsuksakul, P.; Yang, P. *Nat. Nanotechnol.* **2007,** *2*, 435.
(4) Chang, C.-C.; Wu, H.-L.; Kuo, C.-H.; Huang, M. H. *Chem. Mater.* **2008,** *20*, 7570.
(5) Yao, K. X.; Yin, X. M.; Wang, T. H.; Zeng, H. C. *J. Am. Chem. Soc.* **2010,** *132*, 6131.
(6) Lu, W.; Liu, Q.; Sun, Z.; He, J.; Ezeolu, C.; Fang, J. *J. Am. Chem. Soc.* **2008,** *130*, 6983.
(7) Duan, X.; Huang, Y.; Cui, Y.; Wang, J.; Lieber, C. M. *Nature* **2001,** *409*, 66.
(8) Tan, Y.; Xue, X.; Peng, Q.; Zhao, H.; Wang, T.; Li, Y. *Nano Lett.* **2007,** *7*, 3723.
(9) Hernández-Ramírez, F.; Tarancón, A.; Casals, O.; Rodríguez, J.; Romano- Rodríguez, A.; Morante, J. R.; Barth, S.; Mathur, S.; Choi, T. Y.; Poulikakos, D.; Callegari, V.; Nellen, P. M. *Nanotechnology* **2006,** *17*, 5577.
(10) Kuo, C.-H.; Huang, M. H. *J. Phys. Chem. C* **2008,** *112*, 18355.
(11) Ho, J.-Y.; Huang, M. H. *J. Phys. Chem. C* **2009,** *113*, 14159.
(12) Kuo, C.-H.; Huang, M. H. *Nano Today* **2010,** *5*, 106.
(13) Kuo, C.-H.; Hua, T.-E.; Huang, M. H. *J. Am. Chem. Soc.* **2009,** *131*, 17871.
(14) Bao, H.; Zhang, W.; Shang, D.; Hua, Q.; Ma, Y.; Jiang, Z.; Yang, J.; Huang, W. *J. Phys. Chem. C* **2010,** *114*, 6676.
(15) Lyu, L.-M.; Wang, W.-C.; Huang, M. H. *Chem.-Eur. J.* **2010,** *16*, 14167.
(16) Chen, W.-T.; Yang, T.-T.; Hsu, Y.-J. *Chem. Mater.* **2008,** *20*, 7204.
(17) Kamat, P. V. *J. Phys. Chem. C* **2008,** *112*, 18737.
(18) Chen, H.-Y.; Yang, Y.-C.; Lin, H.-W.; Chang, S.-C.; Gwo, S. *Opt. Express* **2008,** *16*, 13465.
(19) Yang, W.-Y.; Rhee, S.-W. *Appl. Phys. Lett.* **2007,** *91*, 232907.
(20) Cheng, G.; Wang, S.; Cheng, K.; Jiang, X.; Wang, L.; Li, L.; Du, Z.; Zou, G. *Appl. Phys. Lett.* **2008,** *92*, 223116.
(21) Sheldon, M. T.; Trudeau, P.-E.; Mokari, T.; Wang, L.-W.; Alivisatos, A. P. *Nano Lett.* **2009,** *9*, 3676.
(22) Zhang, Y.; Deng, B.; Zhang, T.; Gao, D.; Xu, A.-W. *J. Phys. Chem. C* **2010,** *114*, 5073.
(23) Kuo, C.-H.; Huang, M. H. *J. Am. Chem. Soc.* **2008,** *130*, 12815.
(24) Lu, C.; Qi, L.; Yang, J.; Wang, X.; Zhang, D.; Xie, J.; Ma, J. *Adv. Mater.* **2005,** *17*, 2562.
(25) Zheng, Z.; Huang, B.; Wang, Z.; Guo, M.; Qin, X.; Zhang, X.; Wang, P.; Dai, Y. *J. Phys. Chem. C* **2009,** *113*, 14448.